Published online: December 30, 2019

IMR Press

Short Communication

Investigation for the correlation between brain injury and injured ipsilateral sciatic nerve regeneration in a rat model

Haoqi Wang[1], Jianjun Ma[1], Xinze He[2], Qiang Xie[1], Yuting Fu[1] and Pei Wang[1,*]

[1] *Department of Hand & Foot Surgery, Affiliated Hospital of Chengde Medical University, Hebei, Chengde 067000, P. R. China*

[2] *Central Hospital of Binzhou City, Shandong, Binzhou 256600, P. R. China*

*Correspondence: m18631498866@163.com (Pei Wang)

DOI:10.31083/j.jin.2019.04.1155

Previous studies showed that brain trauma promotes repair of peripheral nerve injury by reducing scar in nerve endings. The effect of brain injury at different locations on ipsilateral rat sciatic nerve regeneration in Sprague-Dawley rats was found to promote the repair of ipsilateral sciatic nerve injury, thus providing further experimental evidence for the unveiling of traumatic brain injury promoting peripheral nerve regeneration.

Keywords

Brain injury; neurotrophic factor; peripheral nerves; nerve regeneration; gastrocnemius motor endplate; rat model

1. Introduction

Traumatic brain injury (TBI) is one of the most common clinical traumas, incidence of which is also on rise (Kulbe and Geddes, 2016; Reis et al., 2015). Many studies (Eggers et al., 2016; Li and Cao, 2000; Liu et al., 2013; Yang et al., 2015) have shown that traumatic brain injury could up-regulate the neurotrophic factors, some of which could promote regeneration of peripheral nerve damage, such as neurotrophin-4/5, brain-derived neurotrophic factor. The previous experimental findings indicate that accompanied by the brain injury, regeneration of sciatic nerve injury in rats could be promoted (Zhou et al., 2018). This study aimed to explore whether there are differences in effects of brain injury at different locations on repair and regeneration of sciatic nerve.

Gibson (1960) reported the phenomenon of sciatic nerve repair associated brain injury and fracture healing for the first time. They discovered that femoral fracture associated craniocerebral injury demonstrates more osteophyte formation at the fracture end. Roberts (1968) reported that heterotopic ossification occurs after the brain injury. Subsequently, a large number of experimental studies and clinical observations confirmed that craniocerebral injury could accelerate healing of fractures (Hofman et al., 2015; Wildburger et al., 1994). Meanwhile, the neurotrophins, basic fibroblast growth factors, and the other substances have been proven to play important roles in the pathological processes (Hofman et al., 2015; Wildburger et al., 1994).

A few studies (Pu et al., 1999; Santos et al., 2016) also clarified the effects of rat brain injury on regeneration of a sciatic nerve post the injury. The results demonstrated that sciatic nerve injury with a brain injury demonstrates better functional recovery and neruromorphology compared to that with sciatic nerve injury alone (Pu et al., 1999; Santos et al., 2016). The other studies also showed that when cerebral cortical injury and its corresponding inferior neuronal axon damage at the same time, the expression of some related growth factors are increased and the nerve conduction pathway is also changed (Acosta et al., 2013).

A former study (Lykissas et al., 2007) for traumatic brain injury reported that a major mechanism promoting neuronal repair after brain injury is the up-regulation and release of endogenous neurotrophic factors, such as neurotrophin-4/5, nerve growth factor, basic fibroblast growth factors and brain-derived neurotrophic factors. Peripheral nerve regeneration is a process of axon regeneration and remyelination. This process is affected by many factors, such as microtubule structure. The microtubule structure of basement membrane is composed of extracellular matrix, which could provide molecular guidance signals for regeneration of axons. Schwann cells and neurotrophic factors, such as cell adhesion molecules, could also provide materials and nutritional supports for the axon regeneration. The abundant vascular system could provide sufficient nutrients and oxygen and transport the metabolites. Appropriate physical stimulation can also facilitate activation of neuronal cells and promote growth and development of axon growth cones (Gonzalez-Perez et al., 2013; Homs et al., 2011; Sebben et al., 2011). Then, when the inferior neuron had a certain change due to damage of the superior neuron, its axon regeneration may be affected accordingly. Moreover, Zhou et al. (2018) also reported that accompanied by brain injury, regeneration of sciatic nerve injury in rats could also be promoted. Therefore, this study experimentally designed the sciatic nerve injury model group with ipsilateral and contralateral brain injury, which was used to observe whether there is any difference in effect on functional recovery and histo-morphology of damaged sciatic nerve. Moreover, this study also attempted to explore the relevant mechanisms for the regeneration of peripheral nerve damage in brain-injured rats.

Journal of Integrative Neuroscience

2. Material and methods

2.1 Animals and reagents

This study mainly included the following reagents and equipments: fluorogold (Cat No.: 39286-10MG-F, Sigma-Aldrich, St Louis, MI), acetylthiocholine iodide (Sigma-Aldrich, St Louis, MI), Cryotome (Mode: leica819, Leica, Germany), optimal cutting temperature compound (OCT compound) (Zhengzhou AiGene Biotechnology Co., Ltd., Zhengzhou, P. R. China).

The 99 male specific pathogen free (SPF) Sprague-Dawley (SD) rats, aging 8 weeks, weighting from 220 g to 250 g, were purchased from Beijing Weitong Lihua Experimental Animal Technology Co., Ltd. (Permit No.: SCXK (Beijing) 2012-0001). The rats were kept reared at animal vivarium of affiliated hospital of Chengde medical college. The feeding environment was 20-22 $^{\circ}C$, with free food and drinking water.

2.2 Grouping and processing

A total of 99 SD rats were divided into 3 groups with 33 rats in each group, including group A, group B, and group C, according to the complete randomization method. The group A was assigned as the right sciatic nerve transaction group. The group B was assigned as the right sciatic nerve transaction and right brain injury group. The group C was assigned as the right sciatic nerve transaction and left-brain injury group.

2.3 Establishment of animal models

Sciatic nerve injury model: The sciatic nerve injury model was established according to the previous study described (Das et al., 2017). Briefly, anesthesia was conducted with a volume fraction of 10% chloral hydrate (3.5 mL/kg) intraperitoneally. Postanesthesia, skin preparations were done by disinfecting with alcohol and iodine. Then, the skin was opened in right hip, and the biceps femoris was bluntly separated to expose sciatic nerve. The sciatic nerve was cut approximately 5 mm below the lower hole of piriformis, and then the sciatic nerve was sutured under a microscope with a 10-0 non-invasive suture. Finally, the skin was sutured to close the wound.

Brain injury model: The brain injury model was generated according to the previously published study (Akyol et al., 2018). In brief, the Feeney method was used to establish brain injury models in groups B and C at the same time. Group B received the right brain injury, and group C received a left-brain injury. All rats were given a volume fraction of 10% chloral hydrate (0.35 mL/kg) intraperitoneal injection for anesthesia. The skin was prepared by disinfecting with alcohol and iodine. Sagittal cutting along the head was made to expose the parietal bone. At 1.5 mm behind the coronal line, and 2.5 mm lateral to the midline, a dental drill was used to make a 5 mm diameter bone window, while keeping the dura intact. A 20 g hammer was used to hit the impact rod from a height of 30 cm along the peripheral catheter. After the striker hit the brain tissue, the bone window was closed with bone wax, and the skin was closed by staples.

2.4 Measurements after surgery

All animals were survived after modelling, and no wound infection was found. After the model was established, the right lower limbs of the rats were limited in active flexion. The right foot was deformed, and the foot was healed when walking.

2.5 Measurement and calculation of sciatic nerve function index

At 4, 6, 8, 10, and 12 weeks after modelling, 8 rats in each group were randomly selected to measure and calculate the sciatic nerve function index. The length, breadth, height, and height of wooden channel was 70 cm, 9 cm, 10 cm, respectively. One end was connected to a homemade cassette, and a long strip of white paper of 70 cm × 9 cm was placed at the bottom of the channel. Rats' feet were evenly stained with red ink. From one end, the testing rat walked through the channel into the cassette, and step on the white paper to leave the footprints. After drying, the value was measured. Each rat was measured 3 times at a time, and the average value was taken. The parameters to be measured were listed as the followings: 1 print length (PL): the longest distance from the footprint, i.e., from the heel to the toe; 2 toe spread (TS): from the first to the fifth toe Connection distance; 3 intermediate toe spread (IT): the distance between the 2-4 toe.

Sciatic function index = 38.3 × (EPL - NPL)/NPL + 109.5 × (ETS - NTS)/NTS + 13.2 × (EIT - NIT)/NIT - 8.8 (Yue et al., 2019), where E is the experimental side (right side), N is the healthy side (left side), and the nerve function index S is 0 as the normal value, and -100 is the index of complete nerve dissociation.

2.6 Wet mass of gastrocnemius muscle and calculation of the wet mass ratio

At the 4th, 8th, and 12th week after modelling, 8 rats in each group were randomly selected and anesthetized by intraperitoneal injection of chloral hydrate at a volume fraction of 10%. The calf muscle was incised at the posterior edge of the calf by retrograding from calcaneal tubercle to the femoral condyle. Then, the gastrocnemius muscle was completely removed. The electronic balance was used to weigh the wet mass of gastrocnemius muscle. Then, the wet mass ratio was calculated as the following formula: Wet mass ratio = ipsilateral wet mass of muscle/contralateral wet mass muscle. Post weighting the gastrocnemius muscle mass, the isolated muscle was stored at -80 $^{\circ}C$ for the following analyses.

2.7 Acetylcholinesterase staining of gastrocnemius motor endplates

Preparation of incubation solution (Kamorsky-Roots solution): iodine acetylcholine 12.5 mg (Sigma-Aldrich), 0.1 mol/L sodium dihydrogen phosphate 7 mL, 0.1 mol/L disodium hydrogen phosphate 9 mL, 0.1 mol/L 1 mL of sodium citrate, 2.5 mL of copper sulfate (30 mmol/L), 2.5 mL of 5 mmol/L potassium ferricyanide, and 2 mL of distilled water were added in order and mixed together. The fresh liquid was appeared to be bright green.

Materials acquisition, fixation, sectioning, and staining: The acetylcholinesterase staining was utilized to evaluate gastrocnemius motor plates, according to the previous study recorded (Liu et al., 2013), with a few modifications. Briefly, at 4 weeks, 8 weeks, and 12 weeks, 8 rats in each group were randomly selected (the same rats that were measured for the wet weight of the gastrocnemius muscles), and the volume fraction of chloral hydrate was 10%. The bilateral gastrocnemius muscles were weighed and recorded. Under the microscope, the medial nerve of the right gastrocnemius was taken from the muscle, and the 5 mm tissue section was cut out. The nerve tissue was fixed in 4% formaldehyde for 1 h and then rinsed twice with phosphate buffered saline (PBS) for 3 min each. OCT compound was used to embed the fixed tissue. Approximately 6 μm sections were cut and washed with double

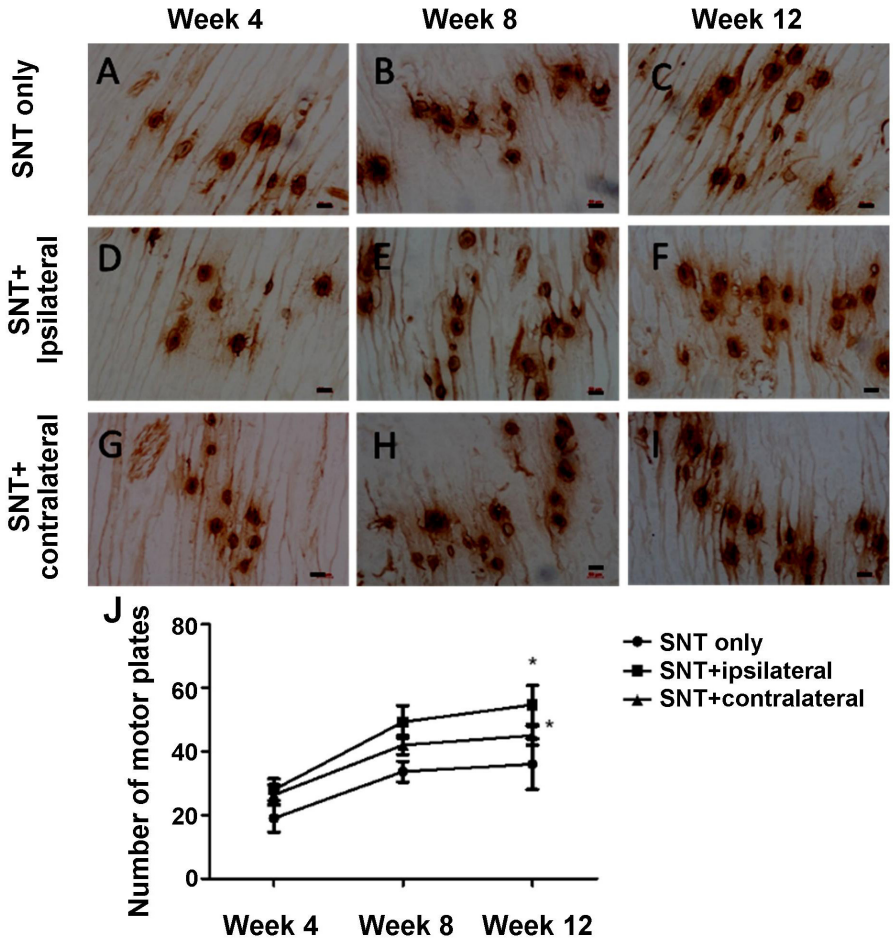

Figure 1. Acetylcholinesterase staining on the rat gastrocnemius in each group. (A-C) The acetylcholinesterase staining of the right end of the sciatic nerve injury group in rats with acetylcholinesterase; (D-F) Sciatic nerve transaction plus ipsilateral brain injury group; (G-I) Sciatic nerve transaction plus contralateral brain injury group. The motor endplates are oval tan particles. As time goes on, the number of motor endplates gradually increases, and the staining increases. (J) Quantification of motor plates marked with acetylcholinesterase staining. * indicated $P < 0.05$ comparing to SNT only group. SNT = sciatic nerve transaction. Scale bar = 50 μm.

distilled water, dried, and sealed with neutral gum. Slides were then observed under the light microscope. Images of the endplate were taken and analyzed with Image-Pro Plus 6.0 to calculate the average absorbance density.

2.8 Fluoro-gold tracing

The fluoro-gold tracing was conducted according to the former study (Puigdellivol-Sanchez et al., 2002), with some modifications. In brief, at 4th, 8th, and 12th week after surgery, 3 rats in each group were randomly selected for the retrograde tracing of fluoro-gold. Fluoro-gold was used to trace L4-L5 vertebrae, and the number of fluoro-gold positive stained spinal cord anterior horn motor neurons was detected and calculated. Anesthesia was administrated in the abdominal cavity with a volume fraction of 10% chloral hydrate. The sciatic nerve was exposed again along the original incision of the right buttock. To ensure the integrity of epineurium, a Fluoro-gold solution (concentration: 4%, dose: 5 μL) was injected into the nerve trunk 5 mm distal to the anastomosis. The needle was kept for 2 min, and was slowly pushed to close the wound layer by layer. After 7 days, the chest of rats was opened to expose the heart under anesthesia. Place the puncture needle in the apex of the heart. Insert the ascending aorta and fix it with silk thread. Cut the right atrial appendage, quickly infuse the normal saline 200-300 mL, and observe the right auricle flowing out of the clear liquid. Then, followed with the injection of 400-500 mL of a 40 g/L paraformaldehyde solution containing 5% sucrose (faster and slower). Subsequently, the right sciatic nerve was exposed, and the spinal cord was opened layer by layer.

The corresponding sciatic nerve was retrogradely positioned in the corresponding spinal segment. L4 and L5 spinal cords were cut out, and some nerve roots were left to identify the right and left. Total of 40 g/L paraformaldehyde solution was used to fix the tissue at 4 $^{\circ}C$ overnight. Then, tissue emerged in 10%, 20%, and 30% sequential sucrose solutions. After that, OCT was used to embed the tissue, and a cryotome was used to cut spinal cord cross-section with thickness of 20 μm. Sections were air-dried, sealed with anti-fluorescence quenching mounting medium, and stored in dark. Observation and counting of fluorescent gold-positive neurons were done under a fluorescence microscope.

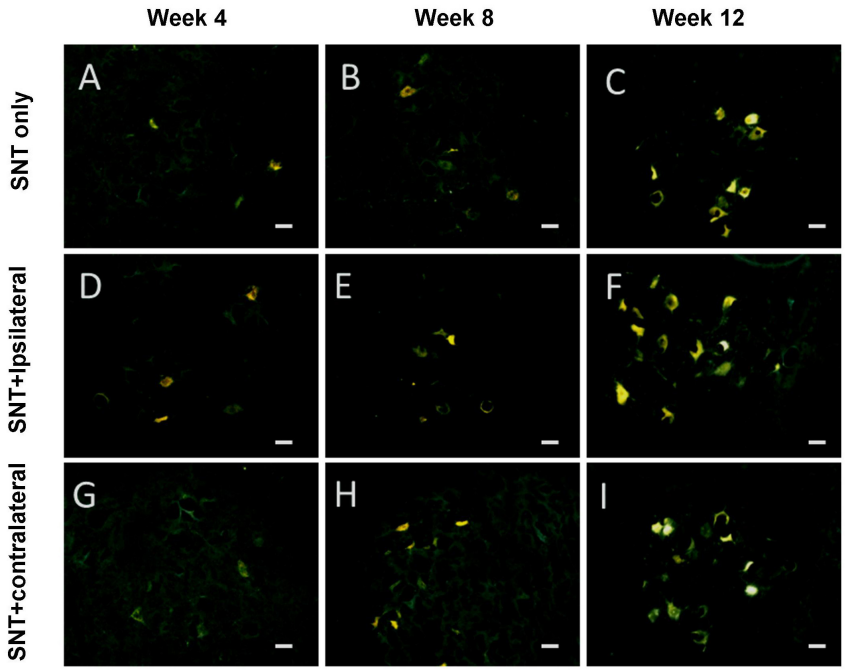

Figure 2. Fluoro-gold staining of the rat spinal cord anterior horn motor neurons (×200). The acetylcholinesterase staining of the right end of the sciatic nerve injury group in rats with acetylcholinesterase. (D-F) Sciatic nerve transaction plus ipsilateral brain injury group. (G-I) Sciatic nerve transaction plus contralateral brain injury group. Golden staining indicates the spinal anterior horn motor neuron that has been traced. As time goes on, the number of axons in the sciatic nerve passing through the lesion increases, and the number of neurons that are tracked increases. SNT = sciatic nerve transaction. Scale bar = 50 μm.

2.9 Motor endplates examination

To identify motor endplate activities, the wholemount acetylcholinesterase (AChE) was employed to stain the muscles of rat models. The isolated and dissected muscles were stained with AChE to identify the distribution and localization for motor endplates of rat models. In brief, staining procedures for wholemount AChE were conducted depended on the previous study reported (Zhang et al., 2011).

2.10 Statistical analysis

All data were assigned as a mean ± standard deviation (SD) and analyzed with SPSS software 19.0 (SPSS Inc., Chicago, Ull, USA). The one-way analysis of variance (ANOVA) followed by post hoc pairwise comparison test was performed for comparing multiple groups. Student's t-test was used to compare the mean of the two groups. $P < 0.05$ means a significant difference.

3. Results

3.1 Sciatic nerve function index

After a prolonged operation, the sciatic nerve function index of each group gradually recovered. In the 4th and 6th weeks, both group B and group C were superior to group A (Table 1), $P < 0.05$). Meanwhile, there was no significant difference between group B and group C (Table 1, $P > 0.05$). At 8 weeks, the recovery of sciatic nerve function index in group B was significantly better compared to that in groups A and C (Table 1, $P < 0.05$).

3.2 Gastrocnemius wet mass ratio

At 4 weeks after modelling, there was no significant difference in the wet weight ratio of the gastrocnemius muscle between 3 groups (Table 2, $P > 0.05$). From the 8th week, the B group was significantly higher compared to that in A and C groups (Table 2, $P < 0.05$).

3.3 Acetylcholinesterase staining of gastrocnemius motor endplate

Acetylcholinesterase staining was performed to detect the endplate of the gastrocnemius muscle. There was no significant difference in the absorbance of the endplate of the gastrocnemius muscle between three groups at 4 weeks after the surgery. From the 8th

Table 1. The rat sciatic functional index in each group at different time points after modeling.

Time (week)	Group A	Group	Group C
4	-78.323 ± 5.203	-69.541 ± 4.118^{a}	-72.181 ± 5.634^{c}
6	-72.936 ± 5.745	-62.924 ± 3.248^{a}	-64.729 ± 4.277^{c}
8	-57.965 ± 6.498	-47.406 ± 3.361^{ab}	-56.106 ± 6.173
10	-51.985 ± 5.659	-37.752 ± 2.852^{ab}	-49..602 ± 6.764
12	-40.113 ± 4.469	-29.794 ± 3.004^{ab}	-36.051 ± 6.158

Group A was a simple right sciatic nerve transaction group. Group B was a right sciatic nerve transaction with a right-brain injury group. Group B was a right sciatic nerve transaction with a left-brain injury group. Compared with group A, $^{a}P < 0.05$. Compared with group C, $^{b}P < 0.05$. Compared with group A, $^{c}P < 0.05$.

Table 2. The wet weight ratio of rat gastrocnemius in each group at different time points after modeling.

Time (week)	Group A	Group B	Group C
4	0.450 ± 0.031	0.528 ± 0.059	0.509 ± 0.068
8	0.507 ± 0.048	0.573 ± 0.047^{ab}	0.537 ± 0.051
12	0.553 ± 0.051	0.682 ± 0.052^{ab}	0.630 ± 0.031

Group A was a simple right sciatic nerve transaction group. Group B was a right sciatic nerve transaction with a right-brain injury group. Group C was a right sciatic nerve transaction with a left-brain injury group. Compared with group A, $^{a}P < 0.05$. Compared with group C, $^{b}P < 0.05$.

Table 3. The absorbance density value of the motor endplate of gastrocnemius at different times after model establishment in rats.

Time (week)	Group A	Group B	Group C
4	0.242 ± 0.056	0.215 ± 0.038	0.221 ± 0.064
8	0.287 ± 0.049	0.339 ± 0.052	0.290 ± 0.062
12	0.313 ± 0.070	0.403 ± 0.121^{ab}	0.336 ± 0.058

Group A is a simple right sciatic nerve transaction group. Group B is a right sciatic nerve transaction with a right-brain injury group. Group C is a right sciatic nerve transaction with a left-brain injury group. Compared with group A, $^{a}P < 0.05$; compared with group C, $^{b}P < 0.05$.

week, the absorbance density of group B was significantly higher compared that of group A and C (Table 3, $P < 0.05$). Also, the number of motor endplates gradually increased, the area gradually increased, and the color also gradually increased (Fig. 1). Quantification of motor endplate confirmed the impression of stained images. The number of motor endplates in group B and group C was significantly more compared to that in group A (Fig. 1J).

3.4 Fluorogold tracing

As shown in Table 4 and Fig. 2, the results of Fluoro-gold retrograde tracing showed that the number of Fluoro-gold staining positive spinal anterior horn motor neurons in groups B and C was significantly higher compared to that in group A at 4 weeks after model establishment ($P < 0.05$). At 8 weeks, the number of Fluoro-gold staining positive neurons was significantly greater in group B compared to that of group A ($P < 0.05$). At 12 weeks, the number of fluorescent gold-positive neurons in group B was significantly higher compared to that in groups A and C ($P < 0.05$). At the same time, group C was more compared to that in group A ($P < 0.05$). Over time, the number of motor neurons marked in the anterior horn of the spinal cord gradually increased.

4. Discussion

In this study, we selected the male rats to establish the traumatic brain injury due to the following reasons: (1) Male rats will be larger in size and weight and easier to operate. (2) The vitality of male rats is stronger. (3) The change of hormone level in male rats is more stable than that in female rats, such as estrogen, growth hormone, etc. (4) Male rats are more sensitive to chronic poisons. The current experimental results showed that the recovery of sciatic nerve function and morphological indexes in group with ipsilateral brain injury are superior to those with contralateral brain injury and sciatic nerve injury alone, with significant differences. The results of the contralateral brain injury group were also significantly better compared to those of the simple sciatic nerve group. In terms of functional performance, as measured by the sciatic nerve function index, which objectively reflected the overall functional recovery of the sciatic nerve, was the most commonly used evaluation for sciatic nerve injury regeneration (Shen and Zhu, 1995). Another parameter to reflect nerve function recovery is the gastrocnemius wet mass ratio. The endplate staining results indirectly reflected the recovery of motor nerve fiber function and the trophic effect on muscle tissue (Ma et al., 2002). Fluorogold tracer reflected the axon regeneration and the recovery of axon transport function, but also indirectly indicated the neuronal function recovery (Catapano et al., 2008). Combined with previous studies and current experimental results, it was presumed that a large number of neurotrophic factors produced by brain injury in two groups of rats with brain injury were the main reasons for the accelerated regeneration of sciatic nerve axons. However, the left cerebral cortex controlled the right sciatic nerve, therefore its injury and the secondary axonal injury adversely affected the secondary motor center, then reduced the promotion of neurotrophic factors and other substances on the sciatic nerve regeneration (Erturk et al., 2016; Kwon and Jang, 2014). Meanwhile, the left cerebral cortex was not damaged for the ipsilateral brain injury group, therefore, the production of neurotrophic factors was more than that in the contralateral brain injury group. Therefore, the contralateral brain injury group was slightly better than that of the sciatic nerve injury group, as well as the ipsilateral traumatic brain injury group was better than that of the contralateral brain injury group for promoting the regeneration of peripheral nerve injury.

In summary, an ipsilateral traumatic brain injury could promote the regeneration of peripheral nerve injury. The possible mechanism may be that the traumatic brain injury induces upregulation of neurotrophic factors, which reversely improve the regeneration of peripheral nerve injury (Werner and Stevens, 2015). Therefore, our future studies will focus on the finding of the relevant neurotrophic factors or growth factors and the determination of the type of neurotrophic or growth factors that play a major

Table 4. The number of rat spinal cord anterior horn motor neurons positive for fluoro-gold in each group.

Time (week)	A group	B group	C group
4	5.800 ± 2.305	6.800 ± 2.077^{a}	6.067 ± 2.052^{c}
8	6.467 ± 2.066	8.733 ± 2.434^{a}	7.067 ± 2.017
12	7.733 ± 2.434	10.933 ± 2.219^{ab}	8.933 ± 2.017^{c}

Group A was a simple right sciatic nerve transaction group; group B was a right sciatic nerve transaction with a right-brain injury group; group C was a right sciatic nerve transaction with a left-brain injury group. Compared with group A, $^{a}P < 0.05$; compared with group C, b = $P < 0.05$; compared with group A, $^{c}P < 0.05$.

role. The present study would provide a theoretical basis for further investigations revealing the therapeutic approaches of traumatic brain injury for treating and promoting the peripheral nerve injury.

Abbreviations

OTC, optimal cutting temperature; PL, print length; TS, toe spread; IT, intermediate toe spread; AChE, acetylcholinesterase; ANOVA, analysis of variance.

Ethics approval and consent to participate

The animal experiments were conducted according to Guidance of Care and Use of Laboratory Animals of National Institutes of Health (NIH). All of the animal experiments were approved by the Ethics Committee of the Affiliated Hospital of Chengde Medical University, Chengde, P. R. China. Approval number: LL037.

Acknowledgement

Thanks to all the peer reviewers and editors for their opinions and suggestions.

Conflict of interest

The authors declare no conflict of interest.

Authors' contributions

HQW and PW designed this study. HQW, JJM, XZH, and QX performed the research. YTF made statistical analyses and conducted the literature review. HQW and PW wrote and revised the manuscript.

Submitted: August 17, 2019
Accepted: December 09, 2019
Published: December 30, 2019

References

Acosta, S. A., Tajiri, N., Shinozuka, K., Ishikawa, H., Grimmig, B., Diamond, D. M., Sanberg, P. R., Bickford, P. C., Kaneko, Y. and Borlongan, C. Y. (2013). Long-term upregulation of inflammation and suppression of cell proliferation in the brain of adult rats exposed to traumatic brain injury using the controlled cortical impact model. *PLoS One* **8**, e53376.

Akyol, O., Sherchan, P., Yilmaz, G., Reis, C., Ho, W. M., Wang, Y., Huang, L., Solaroglu, I. and Zhang, J. H. (2018) Neurotrophin-3 provides neuroprotective via TrkC receptor dependent pErk5 activation in a rat surgical brain injury model. *Experimental Neurology* **307**, 82-89.

Catapano, L. A., Magavi, S. S. and Macklis, J. D. (2008) Neuroanatomical tracing of neuronal projections with Fluoro-Gold. *Methods in Molecular Biology* **438**, 353-359.

Das, S., Sharma, M., Saharia, D., Sarma, K. K., Muir, E. M. and Bora, U. (2017) Electrospun silk-polyaniline conduits for functional nerve regeneration in rat sciatic nerve injury model. *Biomedical Materials* **12**, 045025.

Eggers, R., Tannemaat, M. Rk, De Winter F., Malessy, M. J. and Verhaagen, J. (2016) Clinical and neurobiological advances in promoting regeneration of the ventral root avulsion lesion. *European Journal of Neuroscience* **43**, 318-335.

Erturk, A., Mentz, S., Stout, E. E., Hedehus, M., Dominguez, S. L., Neumaier, E., Krammer, F., Llovera, G., Srinivasan, K., Hansen, D. V., Liesza, A., Scearce-Levie K. A. and Sheng, M. (2016) Interfering with the chronic immune response rescues chronic degeneration after traumatic brain injury. *Journal of Neuroscience* **36**, 9962-9975.

Gibson, J. M. (1960) Multiple injuries: The management of the patient with a fractured femur and a head injury. *Journal of Bone and Joint Surgery* **42**, 425-431.

Gonzalez-Perez, F., Udina, E. and Navarro, X. (2013) Extracellular matrix components in peripheral nerve regeneration. *Inernational Review of Neurobiology* **108**, 257-275.

Hofman, M., Koopmans, G., Kobbe, P., Poeze, M., Aandruszkow, H., Brink, P. R. and Pape, H. C. (2015) Improved fracture healing in patients with concomitant traumatic brain injury: proven or not? *Mediators of Inflammation* **2015**, 204842.

Homs, J., Ariza, L., Pages, G., Udina, E., Navarro, X, Chillon, M. and Bosch, A. (2011) Schwann cell targeting via intrasciatic injection of AAV8 as gene therapy strategy for peripheral nerve regeneration. *Gene Therapy* **18**, 622-630.

Iznak, A. F., Iznak, E. V., Klyushnik, T. P., Kobel'kov, G. M., Damjanovich, E. V., Oleichik, I. V. and Abramova, L. I. (2018) Neurobiological parameters in quantitative prediction of treatment outcome in schizophrenic patients. *Journal of Integrative Neuroscience* **17**, 317-329.

Kulbe, J. R. and Geddes, J. W. (2016) Current status of fluid biomarkers in mild traumatic brain injury. *Experimental Neurology* **275**, 334-352.

Kwon, H. G. and Jang S. H. (2014) Delayed gait disturbance due to injury of the corticoreticular pathway in a patient with mild traumatic brain injury. *Brain Injuiry* **28**, 511-514.

Li, C. Y. and Cao, D. C. (2000) Experimental study on repair of peripheral nerve defect by basic fibroblast growth factor combined with autogenous vein graft conduit. *Zhongguo Xiu Fu Chong Jian Wai Ke Za Zhi* **14**, 14-16. (In Chinese)

Li, Q. G., Huang, Q. M., Liu, L. and Nguyen, T. T. (2019) Structural and functional abnormalities of motor endplates in rat skeletal model of myofascial trigger spots. *Neuroscience Letters* **711**,134417.

Li, R., Liu, Z., Pan, Y., Chen, L., Zhang, Z. and Lu, L. (2014) Peripheral nerve injuries treatment: a systematic review. *Cell Biochemistry and Biophysics* **68**, 449-454.

Liu, H., Wen W., Hu, M., Bi, W., Chen, L., Liu, S., Chen, P. and Tan, X. (2013) Chitosan conduits combined with nerve growth factor microspheres repair facial nerve defects. *Neural Regeneration Research* **8**, 3139-3147.

Lykissas, M. G., Batistatou, A. K., Charalabopoulos, K. A. and Beris, A. E. (2007) The role of neurotrophins in axonal growth, guidance, and regeneration. *Current Neurovascular Research* **4**, 143-151.

Ma, j., Smith, B. P., Smith, T. L., Walker, F. O., Rosencrance, E. V. and Komna, L. A. (2002) Juvenile and adult rat neuromuscular junctions: density, distribution, and morphology. *Muscle and Nerve* **26**, 804-809.

Moore, A. M., Franco, M. and Tung, T. H. (2014) Motor and sensory nerve transfers in the forearm and hand. *Plastic and Reconstructive Surgery* **134**, 721-730.

Pabari, A., Yang, S. Y., Seufalian, A. M. and Mosahebi, A. (2010) Modern surgical management of peripheral nerve gap. *Journal of Plastic, Reconstructive and Aesthetic Surgery* **63**, 1941-1948.

Pu, L. L., Syed, S. A., Reid, M., Patwa, H., Goldstein, J. M., Forman, D. L. and Thomson, J. G. (1999) Effects of nerve growth factor on nerve regeneration through a vein graft across a gap. *Plastic and Reconstructive Surgery* **104**, 1379-1385.

Puigdellivol-Sanchez, A., Valero-Cabre, A., Prats-Galino, A., Navarro, X. and Molander, C. (2002) On the use of fast blue, fluoro-gold and diamidino yellow for retrograde tracing after peripheral nerve injury: uptake, fading, dye interactions and toxicity. *Journal of Neuroscience Methods* **115**, 115-127.

Reis, C., Wang, Y., Akyol, O., Ho, W. M., Li, R. A., Stier, G., Martin, R. and Zhang J. H. (2015) What's new in traumatic brain injury: update on tracking, monitoring and treatment. *International Journal of Molecular Science* **16**, 11903-11965.

Roberts, P. H. (1968) Heterotopic ossification complicating paralysis of intracranial origin. *Journal of Bone and Joint Surgery* **50**, 70-77.

Santos, D., Gonzalez-Perez, F., Giudetti, G., Micera, S., Udina, E., Del Valle, J. and Navarro, X. (2016) Preferential enhancement of sensory and motor axon regeneration by combining extracellular matrix components with neurotrophic factors. *International Journal of Molecular Science* **18**, E65.

Sebben, A. D., Lichtenfels, M. and Da Silva, J. L. (2011) Peripheral nerve regeneration: cell therapy and neurotrophic factors. *Revista Brasileira de Ortopedia* **46**, 643-664.

Shen, N. and Zhu, J. (1995). Application of sciatic functional index in nerve functional assessment. *Microsurgery* **16**, 552-555.

Sun, D., Zhou, R., Dong, A., Sun, W., Zhang, H. and Tang, L. (2016) Nicotine effects on muscarinic receptor-mediated free Ca2+ level changes in the facial nucleus following facial nerve injury. *Journal of Integrative Neuroscience* **15**, 175-190.

Werner, J. K. and Stevens, R. D. (2015) Traumatic brain injury: recent advances in plasticity and regeneration. *Current Opinion in Neurology* **28**, 565-573.

Wildburger, R., Zarkovic, N., Egger, G., Petek, W., Zarkovic, K. and Hofer, H. P. (1994) Basic fibroblast growth factor (BFGF) immunoreactivity as a possible link between head injury and impaired bone fracture healing. *Journal of Bone and Mineral Research* **27**,183-192.

Yang, J., Li, X., Hou, Y., Yang, Y., Qin, B., Fu, G., Qi, J., Zhu, Q., Liu, X. and Gu, L. (2015) Development of a novel experimental rat model for brachial plexus avulsion injury. *Neuroreport* **26**, 501-509.

Yue, L., Talukder, M. A. H., Gurjar, A., Lee, J. I., Noble, M., Dirksen, R. T., Chakkalakal, J. and Elfar, J. C. (2019) 4-Aminopyridine attenuates muscle atrophy after sciatic nerve crush injury in mice. *Muscle and Nerve* **60**, 192-201.

Zhang, X., Mu, L., Su, H. and Sobotka, S. (2011) Locations of the motor endplate band and motoneurons innervating the sternomastoid muscle in the rat. *Anatomical Record* **294**, 295-304.

Zhou, X. B., Zou, D. X., Gu, W., Wang, D., Feng, J. S., Wang, J. Y. and Zhou, J. L. (2018) An experimental study on repeated brief ischemia in promoting sciatic nerve repair and regeneration in rats. *World Neurosurgery* **114**, e11-e21.

Zilic, L., Garner, P. E., Yu, T., Roman, S,, Haycock, J. W. and Wilshaw, S. P. (2015) An anatomical study of porcine peripheral nerve and its potential use in nerve tissue engineering. *Journal of Anatomy 227*, 302-314.